

# Preparation of nickel doped multi-functional micro-patternable polydimethylsiloxane nanocomposite polymer with characterization of its magnetic, electrical and mechanical properties.

A. Khosla <sup>\*</sup>, J. L. Korčok <sup>\*\*</sup>, M. Haiducu <sup>\*\*\*</sup>, B.L. Gray <sup>\*</sup>, D. B. Leznoff <sup>\*\*</sup>, M. Parameswaran <sup>\*\*\*</sup>

<sup>\*</sup> Micro instrumentation Lab, School of Engineering Science, Simon Fraser University, 8888 University Drive, Burnaby, British Columbia, Canada V5A 1S6.

<sup>\*\*</sup> Department of Chemistry, Simon Fraser University, 8888 University Drive, Burnaby, British Columbia, Canada V5A 1S6.

<sup>\*\*\*</sup> IMMR, School of Engineering Science, Simon Fraser University, 8888 University Drive, Burnaby, British Columbia, Canada V5A 1S6.

## ABSTRACT

We present the preparation and characterization of a novel polydimethylsiloxane (PDMS) multifunctional nanocomposite with electric and magnetic properties. The composite is fabricated by ultrasonic agitation of nickel nanoparticles in the PDMS matrix. The prepared nanocomposite is micromolded using conventional soft lithography techniques down to a feature size of 20 $\mu$ m. Microstructures including coils and cantilevers are molded against a poly(methyl methacrylate) mold fabricated via Deep UV LIGA. Nickel polydimethylsiloxane nanocomposites containing up to 45.5 % Nickel nanoparticles by weight in a polydimethylsiloxane matrix demonstrate the largest saturation magnetization of 21.0 emu/g as measured by SQUID magnetometry. It is also observed that the Young Modulus is a linear function of filler loading up to 50 wt% and indicates a material with superior mechanical properties as compared to undoped polydimethylsiloxane. The insulator-conductor transition for the nickel-polydimethylsiloxane composite occurs at 40 wt.%.

**Keywords:** Polydimethylsiloxane, Nanocomposite, Young's Modulus, MEMS, Deep UV LIGA, conductive polymer, magnetic polymer.

## 1 INTRODUCTION

Micro total analysis systems ( $\mu$ TAS), or lab-on-a-chip systems, are microsystems that may contain multiple components for sample preparation, chemical reaction, fluid control, analyte separation and detection, and data acquisition, to accomplish complex tasks such as the detection of disease markers or environmental toxins in

small (e.g., nanoliter) samples of fluid [1]. While many materials have been employed to fabricate microfluidic devices for  $\mu$ TAS, polydimethylsiloxane (PDMS), a silicone based elastomer, has been widely used because of its biocompatibility, low toxicity, high oxidative and thermal stability, optical transparent, low permeability to water, low electrical conductivity, and ease of micropatterning [2]. In order to realize handheld PDMS based  $\mu$ TAS, all of the required components needed by the microsystem must be miniaturized and interconnected into a complete functional system. However, fluid control and data acquisition components may require electrical functionality in addition to fluidic functionality, which may be problematic in PDMS-based microsystems, as adhesion of metals to PDMS is poor and often leads to development of microcracks and electrical failure [3]. Hence, there is a need to develop PDMS-based active materials of similar flexibility to the undoped and insulating PDMS, that can also be easily micromolded using similar soft lithography techniques, to provide robust system electrical routing. In addition, for lab on a chip systems, the ability to manipulate fluid on chip (fluid control) via on-chip microvalves and pumps is usually required [4], with magnetically actuated valves and pumps a good choice due to the high energy density of magnetic actuation schemes [5]. While PDMS is inherently electrically insulating and non magnetic, these properties can be modified by the introduction of conducting and/or magnetic nanoparticles in the polymer matrix. Previously we reported fabrication of electrically conducting PDMS by incorporating multiwalled carbon nanotubes in PDMS matrix [6]. We now report on a different multifunctional material that possesses both electronic and magnetic properties that we characterize, as well as improved mechanical properties, for utilization as electronic routing and magnetic actuation for PDMS-based micro total analysis systems.

## 2 PREPARATION OF MATERIALS AND MICROFABRICATION

### 2.1 Materials

PDMS (Sylgard 184 Elastomer Kit) was purchased from Dow Corning. Nickel nanoparticles with purity of 99.7+% and a diameter of 30-50 nm were obtained from Nanostructure & Amorphous Materials, Incorporated USA. Poly (methyl methacrylate) (PMMA) which is a deep UV photo-patternable polymer was bought from Plaskolite Incorporated USA. All the materials were used as purchased.

### 2.2 Electric and magnetic PDMS preparation

PDMS polymer consists of a base elastomer and curing agent [7] that was manually stirred in 10:1 ratio by weight for 2 minutes. Nickel nanoparticles were ultrasonically dispersed in the prepared PDMS polymer matrix in varying weight percentage by using a VC 750 (Sonic Inc.) programmable ultrasonic processor. The ultra sonic processor was operated in pulse mode (10 seconds on and 15 seconds off cycle) for 2 minutes, which provided mixing by repeatedly allowing the sample to settle back under the probe after each burst. The prepared nanocomposite was placed into a vacuum chamber to remove air bubbles for 30 min prior to micromolding.

### 2.3 Poly(methyl methacrylate) (PMMA) mould microfabrication

PMMA is an excellent choice for a micromolding master due to its high mechanical strength and good dimensional stability. However, the use of PMMA as a positive tone resist or a mold usually involves a highly energetic and very expensive radiation source. One classical example is the use of synchrotron light (x-ray) for LIGA [8-11]. LIGA is a German acronym, standing for **L**ithographie, **G**alvanoformung, **A**bformung which translates to lithography, electroplating, and molding, for which the high cost x-ray source is required for the lithographic aspects of the process. However, it has been demonstrated that PMMA patterning with a latent image can be accomplished using low-pressure mercury (germicidal) lamps [12-14], thus reducing drastically the cost associated with PMMA lithography. We utilize this low-cost, deep-UV lithography process for the fabrication of our molds.

Figure 1 shows the basic fabrication sequence. The chosen structural material for the micromold was OPTIX<sup>®</sup>, a commercial acrylic purchased from Plaskolite. The irradiation source was a Stratalinker 2400UV crosslinker equipped with five low-pressure mercury lamps able to

provide a nominal power of 4mW/cm<sup>2</sup> and a deep-UV spectrum with a maximum peak at 253.7 nm. In photolithography, collimated light is required for high aspect ratio patterning. However, the Stratalinker provides uncollimated illumination. To improve the resulting aspect ratio a plastic grate made of 12.5 by 12.5 mm squares, each with a height of 13 mm, was set at a distance of 2 cm above the substrates during exposure. This way, only the light that hits the bottom plane of the grate at angles less than 46° with respect to the perpendicular on the surface are allowed through. Further, to even out the irradiation so that no square patterns are formed as a result of positioning the grate above the substrates, the latter were set on top of a rotational stage driven by a dc motor, which was fed by a 9 Volt battery. The rotational frequency of the stage was approximately 0.125 Hz.

Prior to the following succession of steps, the acrylic was cut into 3 x 3 inch squares, cleaned with water and methanol, and then dried with a stream of nitrogen gas. A hard metal mask of 100nm of gold was sputtered on the PMMA substrate using a Corona Vacuum System sputterer. After metal deposition, Shipley 1813 photoresist was spun on at 4000rpm for 30 seconds. Because the PMMA may warp if baked above 100°C, the photoresist baking temperature was kept below 75°C. The sample was exposed through a contact mask using an i-line source and developed in MF-319. The hard mask was etched using TFA gold etchant from Transene Company, Inc. Following the gold etch, the photoresist was removed using a 60 second blanket exposure followed by another development in MF-319, thus avoiding damage to the OPTIX<sup>®</sup> by strong organic solvents such as acetone or photoresist stripper typically used to remove photoresist. At this point, the samples were exposed to deep UV using the hard mask for patterning, using a dose of 6650 Joules.

The samples were immersed in a developer bath consisting of 7:3 isopropyl alcohol (IPA) to de-ionized water (DI water) at 28°C for 1 hour. The temperature was maintained constant throughout the development and the bath was given a slight manual agitation. The development of the samples was quenched in an ultrasonic IPA bath at room temperature (~18°C) for 10 seconds, followed by an IPA rinse for another 10 seconds. This quenching was necessary to prevent the re-deposition of the partially dissolved PMMA. After removing the gold mask using TFA gold etchant, rinsing with DI water, and blowing the samples dry with nitrogen gas, the depth of the etched channels were measured using an Alpha-step 500 profilometer and found to be 100µm deep and a width of 20µm.

### 2.4 Micromolding

Micromolding was accomplished using standard soft lithography methods as is typically utilized for undoped

PDMS [15]. The Ni-PDMS nanocomposites with different doping levels were prepared as defined in section 2.2 and poured on the PMMA molds prepared as discussed in section 2.3. The excess PDMS on the PMMA mould was scraped off using a glass slide and then de-gassed to remove any air bubbles for 30 minutes. The samples were baked on a hot plate at a temperature of 75 °C for 1 h followed by cooling to room temperature. The structures were then peeled off from the mold and were ready for testing. Figure 2 shows examples of resulting Ni-PDMS microfabricated structures

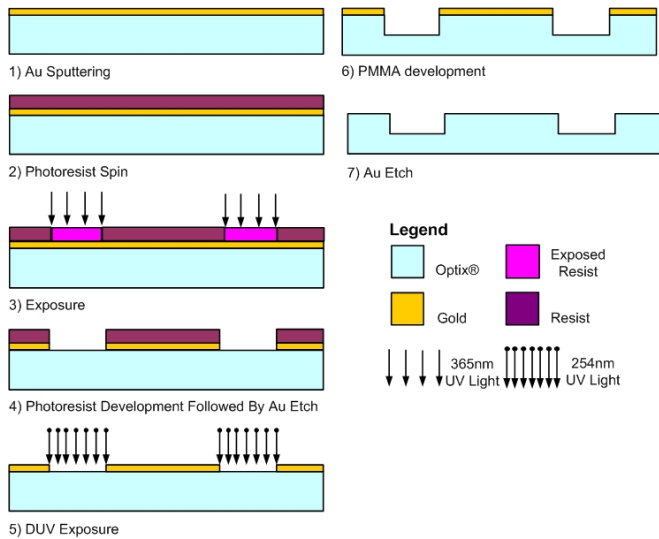


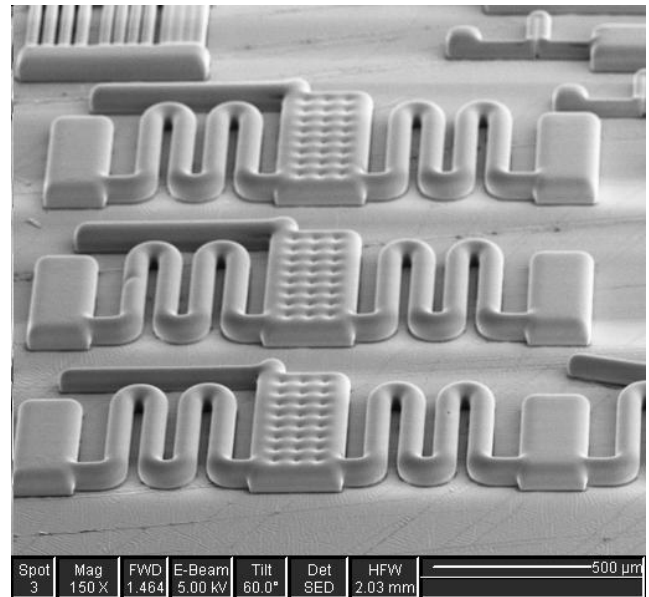
Figure 1: Deep-UV exposure of PMMA: fabrication process steps

### 3 EXPERIMENTAL RESULTS AND DISCUSSION

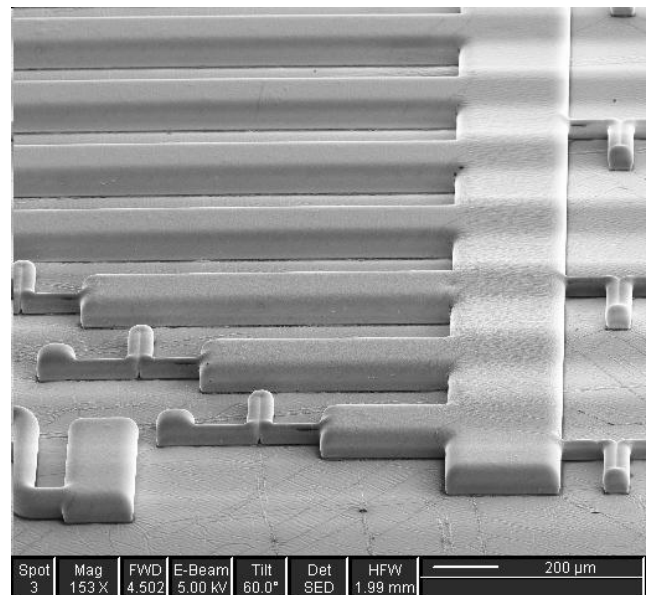
#### 3.1 Magnetic characterization

Magnetic properties of Ni-PDMS nanocomposites were analyzed by SQUID magnetometry and were compared to the pure nickel nanoparticles. Magnetometry measurements were carried out on a Quantum Design MPMS-XL-7S SQUID magnetometer equipped with an Evercool liquid helium dewar. Ni-PDMS samples, as well as the pure (30-50 nm) Ni nanoparticles, were packed in polycarbonate capsules and mounted in low-background diamagnetic straws. For each sample, magnetization ( $M$ ) vs. field ( $H$ ) hysteresis measurements were obtained at 300 K in fields between +2 T and -2 T, taking data every 25-200 G at low fields ( $< 0.2$  T) and 1000-5000 G at higher fields. The pure Ni nanoparticles were found to have a saturation magnetization,  $M_{sat}$ , of 46.0 emu/g. The coercivity,  $H_c$ , is 105 G, indicating that the material is a soft magnet. The shapes of the hysteresis fields loops, fields at which saturation occurs, and coercive fields are nearly identical for all Ni-

PDMS composites, verifying that the incorporation of the



(a)



(b)

Figure 2: Scanning Electron Microscopy (SEM) images (a) Bridges (b)Micromolded cantilevers

nanoparticles into PDMS films did not change their fundamental magnetic properties. As expected,  $M_{sat}$  values per gram of nanocomposite correlate linearly with the weight percent of Ni in PDMS (Figure 3), with the 45.5 % sample having the largest saturation magnetization, at 21.0 emu/g as compared to the pure Ni Nanoparticles which had a saturation magnetization of 45.7 emu/g (shown in Figure 3 as the 100 wt% point).

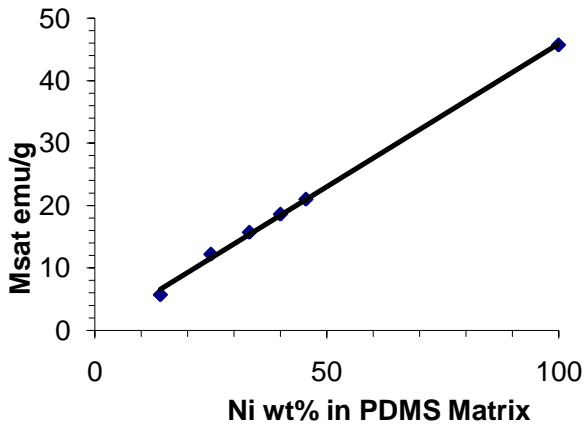


Figure 3: Saturation magnetization ( $M_{sat}$ ) per gram of composite as a function of mass percent of Ni in the Ni-PDMS composites.

### 3.2 Mechanical characterization

Young's Modulus measurements were done using an Instron +3340 Series Single Column System. A total of ten test specimens were fabricated with varying weight percentage of nickel nanoparticles in PDMS (eg. 0, 14.06, 25, 30 ...55), with each sample having a gage length of 75 mm, a width of 25 mm, and a thickness of 1mm. Tests were carried out employing the ASTM (E8-04) Standard Test Method. After the sample was loaded into the testing apparatus and the strain gage attached to the specimen, all variables were cleared and the speed of the grips was set to 15 mm/minute. Each specimen was pulled until failure while data was collected by a computer acquisition system. The measured Young's Modulus of pure PDMS was found to be 0.59 MPa, which lies well within the range of earlier reported values of 0.36-0.87 MPa [16]. Figure 4 shows results of Young's Modulus for all fabricated nanocomposites. The Young's Modulus increases with increasing Wt% of nickel nanoparticles in the PDMS matrix. Thus, doping the PDMS with nickel nanoparticles results in materials with higher Young's Modulus. However, after 60 Wt% the nanocomposite could not be easily micromolded because of increased viscosity at high fill levels. It was observed that the Young Modulus's is an approximately linear function of filler loading up to 50 wt%, and can be particularly enhanced. The curve levels off slightly above 50 wt%, although still increases. The results obtained are in accordance with the experimental values previously reported by other researchers on nanocomposite polymers doped with 200nm silver [17].

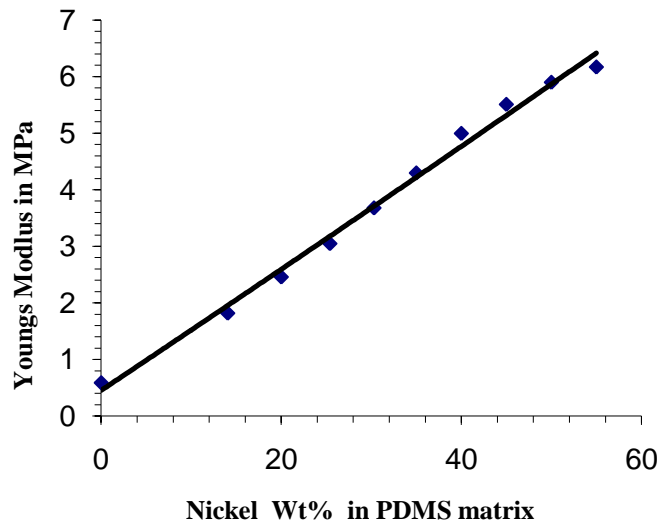


Figure 4: Young Modulus's versus nickel weight percentage (Wt%) in PDMS matrix

### 3.3. Electrical characterization

The direct current (DC) electrical properties of 10 mm x 5mm x 1mm films of the Ni-PDMS nanocomposite were measured using an HP3748A digital multimeter, which was set to operate in a four probe mode to eliminate the contact resistance. Figure 5 shows the resulting resistivity of nickel nanoparticle doped PDMS with varying weight percentage. It can be clearly seen that the resistivity decreases with increasing nickel nanoparticle weight percentage. It is observed that up to 40 weight percent the resistivity decreases slowly. However, after this point, which is the percolation threshold, the resistivity decreases rapidly and can be explained in terms of percolation theory [18]. At

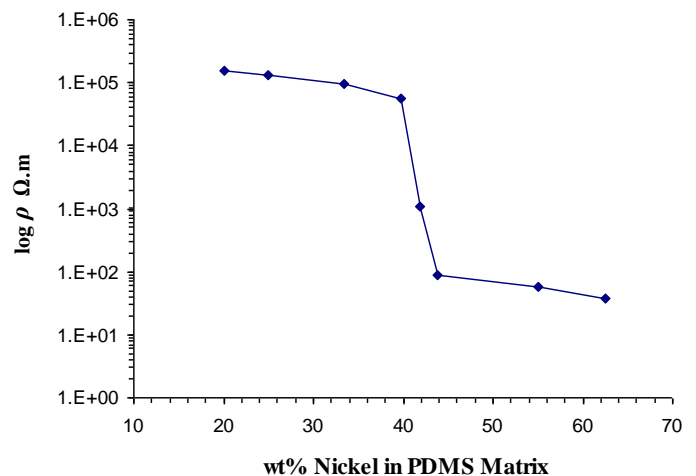


Figure 5: Resistivity versus nickel wt % in PDMS matrix

lower concentrations the nickel nanoparticle percolation paths are not set up and as the concentration is increased the percolation paths are set up by the conducting nickel nanoparticles. At this point the nickel nanoparticles control the conductivity of the nanocomposite. The percolation threshold was observed to be equal to 41 wt% for the Ni-PDMS nanocomposite.

## 4 CONCLUSION

The electrical, magnetic and mechanical properties of micropatternable nickel nanoparticle (30-50nm) doped polydimethylsiloxane have been characterized as a function of weight percentage of nickel nanoparticles in the PDMS matrix. It is observed that a percolation threshold occurs at approximately 40 weight percentage and the highest saturation magnetization occurs at 45.2 weight percentage. It was also observed that beyond 60 weight percentage, the nanocomposite becomes difficult to micropattern. The fabricated nanocomposite has superior mechanical properties, with a higher Young's Modulus than undoped PDMS; the relationship between Young's Modulus and nanoparticle doping was found to be approximately linear. We have been successfully able to micromold the prepared nanocomposite down to feature sizes of 50 $\mu$ m (limited by the photomask resolution limit), using a fabrication process similar to unfilled PDMS [19]. The multifunction material can be not only used to solve the signal routing problem in  $\mu$ TAS but also shows promise as a magnetically actuated material for fluid control components such as microvalves and pumps. Further work will involve incorporating this novel material in developing microheaters, microvalves and micropumps for all polymer in lab on a chip devices.

## ACKNOWLEDGEMENTS

The authors would like to acknowledge NSREC for Discovery Grant funding; CMC Microsystems for providing us with tools for mask design; and CFI and BCKDF for providing funds for the polymer microstructuring facility. SERC (DBL, JLK) and the SQUID magnetometer facility was also funded by CFI and BCKDF. We would also like to thank Bill Woods for help with microfabrication.

## REFERENCES

- [1] George M. Whitesides, NATURE, Vol 442, 27 July 2006.
- [2] Younan Xia and George M. Whitesides, Annu Rev Mater Sci **28** (1998), pp. 153–184
- [3] A.J Gallant.; D.A Zeze; D Wood,.; M.C Petty, D. Dai; J.M Chamberlain, Infrared and Millimeter

- Waves, 2007 and the 2007 15th International Conference on Terahertz Electronics. IRMMW-THz., vol., no., pp.982-983, 2-9 Sept. 2007
- [4] Petra S Dittrich, Kaoru Tachikawa, Andreas Manz, Analytical Chemistry, Vol. 78, No. 12. (1 June 2006), pp. 3887-3908.
- [5] Nicole Pamme, Critical Review: Lab Chip, 2006, 6, 24 – 38
- [6] A. Khosla and B. L. Gray, [Materials Letters Volume 63, Issues 13-14](#), 31 May 2009, Pages 1203-1206.
- [7] <http://www.dowcorning.com/applications/search/products/Details.aspx?prod=01064291&type=PROD&hcp=1>.
- [8] Becker, E.W., et al., Microelectronic Engineering, 1986. **4**(1): p. 35-36.
- [9] Ehrfeld, W. and D. Münchmeyer, Nuclear Instruments and Methods in Physics Research A, 1991. **303**(3): p. 523-531.
- [10] Ehrfeld, W. and H. Lehr, Radiation Physics and Chemistry, 1995. **45**(3): p. 349-365.
- [11] Achenbach, S., Klymyshyn D, Haluzan D, Mappes T, Wells G, Mohr J., Microsystem Technologies, 2006. **13**(3-4): p. 343-347.
- [12] M Haiducu, M Rahbar, I G Foulds, RW Johnstone, D Sameoto and M Parameswaran Journal of Micromechanics and Microengineering, 2008. **18**(11): p. 115029-115036.
- [13] Johnstone, R., I.G. Foulds, and M. Parameswaran, Journal of Vacuum Science and Technology B, 2008. **26**(2): p. 682-685.
- [14] Johnstone, R.W., I.G. Foulds, and M. Parameswaran. Proceedings of the Canadian Conference on Electrical and Computer Engineering (2007). CCECE 2007. Vancouver, BC, Canada: IEEE
- [15] S. Jaffer and B.L. Gray, J Micromechanics Microengineering **18** (2008), p. 035043.
- [16] <http://www.mit.edu/~6.777/matprops/pdms.htm>
- [17] P McCluskey,.; Nagvanshi, M.; Verneker, V.R.P.; Kondracki, P.; Finello, D., Proceedings of 3rd International Conference on Adhesive Joining and Coating Technology in Electronics Manufacturing, 1998, p 282-6.
- [18] B.J. Last and D.J. Thouless, Phys Rev Lett **27** (1971), pp. 1719–1721.
- [19] S.M. Westwood, S. Jaffer and B.L. Gray, J Micromechanics Microengineering **18** (2008), p. 064014 (9 pp.)